Pharmaceutical Research, Vol. 23, No. 6, June 2006 (© 2006)
DOI: 10.1007/s11095-006-0204-y

Research Paper

Intestinal Absorptive Transport of the Hydrophilic Cation Ranitidine: A Kinetic Modeling Approach to Elucidate the Role of Uptake and Efflux Transporters and Paracellular *vs.* Transcellular Transport in Caco-2 Cells

David L. Bourdet,[1] Gary M. Pollack,[2] and Dhiren R. Thakker[1,3]

Received July 15, 2005; accepted February 8, 2006

Purpose. The mechanism of intestinal drug transport for hydrophilic cations such as ranitidine is complex, and evidence suggests a role for carrier-mediated apical (AP) uptake and saturable paracellular mechanisms in their overall absorptive transport. The purpose of this study was to develop a model capable of describing the kinetics of cellular accumulation and transport of ranitidine in Caco-2 cells, and to assess the relative contribution of the transcellular and paracellular routes toward overall ranitidine transport.

Methods. Cellular accumulation and absorptive transport of ranitidine were determined in the absence or presence of uptake and efflux inhibitors and as a function of concentration over 60 min in Caco-2 cells. A three-compartment model was developed, and parameter estimates were utilized to assess the expected relative contribution from transcellular and paracellular transport.

Results. Under all conditions, ranitidine absorptive transport consisted of significant transcellular and paracellular components. Inhibition of P-glycoprotein decreased the AP efflux rate constant (k_{21}) and increased the relative contribution of the transcellular transport pathway. In the presence of quinidine, both the AP uptake rate constant (k_{12}) and k_{21} decreased, resulting in a predominantly paracellular contribution to ranitidine transport. Increasing the ranitidine donor concentration decreased k_{12} and the paracellular rate constant (k_{13}). No significant changes were observed in the relative contribution of the paracellular and transcellular routes as a function of ranitidine concentration.

Conclusions. These results suggest the importance of uptake and efflux transporters as determinants of the relative contribution of transcellular and paracellular transport for ranitidine, and provide evidence supporting a concentration-dependent paracellular transport mechanism. The modeling approach developed here may also be useful in estimating the relative contribution of paracellular and transcellular transport for a wide array of drugs expected to utilize both pathways.

KEY WORDS: drug transporters; intestinal absorption; mathematical modeling; paracellular transport; transcellular transport.

INTRODUCTION

Intestinal drug absorption occurs via either the transcellular or paracellular pathway. Transcellular absorption is generally the preferred route for orally administered drugs and is governed by simple passive diffusion for sufficiently lipophilic molecules or carrier-mediated transport mechanisms for compounds that can serve as substrates for intestinal transporters. Numerous intestinal uptake and efflux transporters have been implicated in facilitating or hindering absorption of a wide array of drugs [e.g., PepT1 and P-glycoprotein (P-gp) substrates] that utilize the transcellular pathway. In contrast, absorption via the paracellular route is typically restricted by the relatively small pore size of the paracellular canal and the presence of the tight junction that acts as a barrier to drug absorption. Despite these limitations, paracellular transport may be an important absorption mechanism for hydrophilic drugs that exhibit poor membrane permeability and that do not serve as substrates for intestinal uptake carriers.

The H_2 receptor antagonist ranitidine is a well-absorbed drug despite its hydrophilic nature, a net positive charge, and a large number of hydrogen bonding sites. Recent studies in the Caco-2 cell culture model of intestinal epithelium have suggested that absorptive transport of ranitidine across the cell monolayers occurs via a complex mechanism involving both passive diffusion and a saturable organic cation uptake

[1] Division of Molecular Pharmaceutics, School of Pharmacy, The University of North Carolina at Chapel Hill, Kerr Hall, CB #7360, Chapel Hill, North Carolina 27599-7360, USA.
[2] Division of Pharmacotherapy and Experimental Therapeutics, School of Pharmacy, The University of North Carolina at Chapel Hill, Kerr Hall, CB #7360, Chapel Hill, North Carolina 27599-7360, USA.
[3] To whom correspondence should be addressed. (e-mail: dhiren_thakker@unc.edu)

ABBREVIATIONS: AP, apical; BL, basolateral; k_{12}, AP uptake rate constant; k_{13}, paracellular rate constant; k_{21}, AP efflux rate constant; k_{23}, BL efflux rate constant; k_{32}, BL uptake rate constant; $P_{app,para}$, paracellular permeability; $P_{app,total}$, total permeability; $P_{app,trans}$, transcellular permeability; P-gp, P-glycoprotein.

transporter that is attenuated by P-gp-mediated apical (AP) efflux (1). In contrast, previous investigations have suggested that absorptive transport of ranitidine across Caco-2 cell monolayers occurs predominantly via the paracellular route (2–4). The evidence for paracellular transport in these studies was based on the observation that the absorptive transport of ranitidine increased severalfold when the intercellular tight junctions were breached by removal of extracellular Ca^{2+}. The experimental design of these studies makes it difficult to discriminate between compounds that solely utilize the paracellular pathway (e.g., mannitol) and those that exhibit varying degrees of transcellular transport (i.e., due to limited membrane permeability or low-efficiency carrier-mediated transport). Furthermore, such experiments are not truly quantitative and do not allow an assessment of the relative contribution of the transcellular and paracellular pathways to the overall transport. Thus, the relative contribution of each pathway for hydrophilic compounds, such as ranitidine, that exhibit carrier-mediated uptake across the AP membrane as well as paracellular transport is largely unknown.

Several approaches have been developed to estimate the relative contribution of the transcellular and paracellular pathways to intestinal drug transport. Adson *et al.* developed a model utilizing the theory of molecular size-restricted diffusion of cations and anions within a negative electrostatic field of force to predict paracellular permeability in cultured epithelial cells (5,6). Using the overall effective absorptive permeability across the monolayer, their model has been used to uncouple the transcellular and paracellular permeabilities for several model compounds (6,7). Another approach utilized a combined parallel artificial membrane permeation assay (PAMPA) and transport across Caco-2 cell monolayers to estimate the contribution of each pathway. This approach assumed the transcellular permeability to be equivalent to the PAMPA permeability; and the paracellular permeability was determined by the difference between the observed Caco-2 and PAMPA permeabilities (8). Other recent approaches have investigated transport of charged species as a function of pH in multiple cell culture systems with varying degrees of paracellular leakiness to determine paracellular permeabilites of hydrophilic ionic compounds (9). Each of these approaches attempts to estimate the contribution from two parallel and competing pathways (i.e., transcellular and paracellular) in the translocation of compounds across cell monolayers by using data solely obtained from the appearance of compound in the receiver [basolateral (BL)] compartment and by combining data from multiple model systems. Such approaches involve extrapolating the behavior of compounds from one system [i.e., transport across electrostatic field of charge, continuous membrane sheets (PAMPA)] to the cell culture system (e.g., Caco-2 cells) in which the relative contribution of the two pathways is being assessed.

In this report, a compartmental kinetic modeling approach was utilized to estimate the contribution of the transcellular and paracellular pathways to the absorptive transport of ranitidine. The multiexperimental approach employed relies on a kinetic evaluation of the discrete transmembrane events occurring at the AP and BL domains in addition to the overall transport across the cell monolayers, and integrates these parameters into a cellular kinetic model that best describes these processes. Using this approach, one could determine the contribution of the paracellular and transcellular routes in the absorptive transport of ranitidine across Caco-2 cell monolayers. The studies reported here demonstrate that the transcellular transport of ranitidine is defined by an interplay between absorptive organic cation transporter(s) and apically directed efflux mediated by P-gp, and provide support for the existence of a concentration-dependent paracellular absorptive transport mechanism for ranitidine.

MATERIALS AND METHODS

Materials

The Caco-2 cell line, Caco-2 cell clone P27.7 (10), was obtained from Mary F. Paine, Ph.D., and Paul B. Watkins, M.D. (Schools of Pharmacy and Medicine, The University of North Carolina at Chapel Hill, Chapel Hill, NC, USA). Eagle's minimum essential medium (EMEM) with Earle's salts and L-glutamate, nonessential amino acids (NEAA, 100×), 0.05% trypsin–0.53 mM EDTA solution, and penicillin–streptomycin– amphotericin B solution (100×) were obtained from Gibco Laboratories (Grand Island, NY, USA). Fetal bovine serum (FBS) was obtained from Sigma Chemical Co. (St. Louis, MO, USA). Hank's balanced salt solution (HBSS) was obtained from Mediatech, Inc. (Herndon, VA, USA). *N*-Hydroxyethylpiperazine-*N′*-2-ethanesulfonate (HEPES, 1 M) was obtained from Lineberger Comprehensive Cancer Center at the University of North Carolina at Chapel Hill. Ranitidine was purchased from Research Biochemicals International (Natick, MA, USA). Quinidine was purchased from Sigma. GW918 (11) was obtained as a gift from GlaxoSmithKline (Research Triangle Park, NC, USA).

Cell Culture

Caco-2 cells were cultured at 37°C in EMEM supplemented with 10% FBS, 1% NEAA, 100 U/mL penicillin, 100 μg/mL streptomycin, and 0.25 μg/mL amphotericin B in an atmosphere of 5% CO_2 and 90% relative humidity as described previously (1).

Transport and Cellular Accumulation Studies

Transport and cellular accumulation studies were conducted as described previously with minor deviations (1). Transport experiments were initiated by replacing the donor solution (AP for absorptive transport) with 0.4 mL of transport buffer containing ranitidine (0.1, 0.5, or 2 mM) or ranitidine (0.1 mM) in the presence of GW918 (1 μM) or quinidine (200 μM). Transport experiments were terminated at the indicated time points, and the appearance of ranitidine in the receiver compartment (BL) as well as cellular accumulation was determined as previously described (1). GW918 (1 μM) was added to the incubation medium, donor, and receiver solutions in studies investigating inhibition of

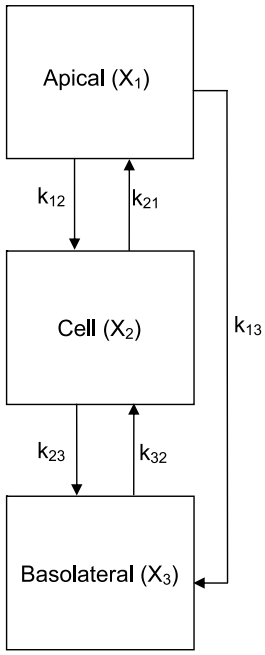

Fig. 1. Schematic representation of the three-compartment model describing the transport of ranitidine in the Caco-2 cell model. Compartments represent the AP (X_1), cellular (X_2), and BL (X_3) chambers. Rate constants associated with transmembrane flux are denoted as follows: AP uptake (k_{12}), AP efflux (k_{21}), BL uptake (k_{32}), and BL efflux (k_{23}). k_{13} represents the rate constant associated with paracellular transport.

P-gp. Transepithelial electrical resistance (TEER) was measured at the beginning and end of each experiment to ensure monolayer integrity throughout the course of the experiment. Cell monolayers with final TEER $\leq$ 300 Ω cm^2 were discarded.

High-Performance Liquid Chromatography Analysis

The amount of ranitidine transported or accumulated in the Caco-2 cells was quantified by high-performance liquid chromatography (HPLC, Agilent Technologies, 1100 Series, Palo Alto, CA, USA) using a 100 $\times$ 3 mm C18 Aquasil column (5 μm; Keystone Scientific, Inc. Bellefonte, PA, USA) as previously described (1).

Mathematical Model

A compartmental modeling approach was utilized to examine the accumulation and absorptive transport of ranitidine in Caco-2 cells. The three-compartment model structure is depicted in Fig. 1. Differential equations based on the model structure in Fig. 1 and describing the transfer of mass between compartments are as follows:

$$\frac{dX_1}{dt} = -(k_{12} + k_{13}) \cdot X_1 + k_{21} \cdot X_2 \quad (1)$$

$$\frac{dX_2}{dt} = k_{12} \cdot X_1 - (k_{21} + k_{23}) \cdot X_2 + k_{32} \cdot X_3 \quad (2)$$

$$\frac{dX_3}{dt} = k_{23} \cdot X_2 + k_{13} \cdot X_1 - k_{32} \cdot X_3 \quad (3)$$

where X_1, X_2, and X_3 represent the amount of drug in the AP, cellular, and BL compartments, respectively. First-order rate constants (min^{-1}) denote parameters associated with AP uptake (k_{12}), AP efflux (k_{21}), BL uptake (k_{32}), BL efflux (k_{23}), and paracellular transport (k_{13}). Preliminary modeling indicated a parameter associated with reverse paracellular flux (k_{31}) did not contribute significantly to absorptive transport of ranitidine, probably due to the large AP to BL concentration gradient and the time course imposed by the conditions of the experiment. Therefore, this parameter was removed from subsequent modeling exercises. Parameter estimates were obtained by fitting the model to the overall ranitidine transport and cellular accumulation data simultaneously using nonlinear least-squares regression (WinNonlin, Pharsight, Mountain View, CA, USA). A weighting scheme of $1/Y$ and the Gauss-Newton (Levenberg and Hartley) minimization method were used for each modeling exercise. In some cases, parameter estimates for AP uptake (k_{12}) and BL uptake (k_{32}) were fixed during nonlinear regression at experimentally determined values. Fixed parameters allowed recovery of more accurate parameter estimates for the variable parameters under specific experimental conditions. The rate constants (k_{12} and k_{32}) were calculated by using the kinetic parameters (J_{max}, K_m, and K_d) associated with AP and BL uptake determined previously (Table I) (1, 12) and according to the following equations:

$$\frac{dX_2}{dt_{initial}} = k_{12(or\,32)} \cdot X_{1(or\,3)} \quad (4)$$

where $dX_2/dt_{initial}$ is the initial rate of uptake into the cell. The rate of initial uptake can also be described as:

$$\frac{dX_2}{dt_{initial}} = \frac{J_{max} \cdot X_{1(or\,3)}}{K_m + X_{1(or\,3)}} + \frac{K_d \cdot X_{1(or\,3)}}{V_{AP(or\,BL)}} \quad (5)$$

where J_{max} is the maximal uptake rate, K_m is the Michaelis-Menten constant, K_d is the nonsaturable component of uptake, and $V_{AP\ (or\ BL)}$ is the volume of the donor compartment (AP, 400 μL; BL, 1500 μL). It should be noted that the amount of ranitidine [$X_{1\ (or\ 3)}$] is expressed as a mass (e.g., picomoles) and not in terms of concentration. K_m, therefore,

Table I. Kinetic Parameters for Apical (AP) and Basolateral (BL) Uptake of Ranitidine in Caco-2 Cells

Uptake direction	J_{max} [pmol min^{-1} (mg protein^{-1})][a]	K_m (mM)	K_d [μL min^{-1} (mg protein^{-1})][a]
AP[b]	680	0.45	0.264
BL[c]	20,900	66.9	n/a[d]

[a] Calculation of k_{12} and k_{32} required multiplication of the reported J_{max} and K_d values by the average protein content of the monolayers (0.20 mg protein).
[b] Kinetic parameters for AP uptake were previously reported (1).
[c] Kinetic parameters for BL uptake were previously reported (12).
[d] BL uptake data did not support the incorporation of a term for nonsaturable uptake. n/a: not applicable.

is also expressed in terms of mass and converted from concentration by multiplying by the volume of the donor compartment. Substitution of Eq. (5) into Eq. (4) enables calculation of the rate constant from the experimentally determined kinetic parameters as follows:

$$k_{12(or\,32)} = \frac{J_{max}}{K_m + X_{1(or\,3)}} + \frac{K_d}{V_{AP(or\,BL)}} \quad (6)$$

J_{max} and K_d values were normalized for protein content of the monolayers. Calculation of the rate constants (min^{-1}) thus involved multiplication of the J_{max} and K_d values by the average protein content of the monolayers (0.20 mg protein).

Simulation of Transcellular and Paracellular Transport

The transcellular and paracellular contributions to overall ranitidine transport were determined by utilizing the parameter estimates obtained from kinetic modeling and simulating the appearance of ranitidine in the BL compartment by using subsets of the original kinetic model that incorporated solely paracellular or transcellular components. Equations used for simulations were as follows:

Paracellular:

$$\frac{dX_1}{dt} = -k_{13} \cdot X_1 \quad (7)$$

$$\frac{dX_3}{dt} = k_{13} \cdot X_1 \quad (8)$$

Transcellular:

$$\frac{dX_1}{dt} = -k_{12} \cdot X_1 + k_{21} \cdot X_2 \quad (9)$$

$$\frac{dX_2}{dt} = k_{12} \cdot X_1 - (k_{21} + k_{23}) \cdot X_2 + k_{32} \cdot X_3 \quad (10)$$

$$\frac{dX_3}{dt} = k_{23} \cdot X_2 - k_{32} \cdot X_3 \quad (11)$$

Data Analysis

Data are expressed as mean ± SD from three measurements unless otherwise noted. Apparent permeability (P_{app}) was determined from Eq. (12):

$$P_{app} = \frac{dQ/dt}{AC_o} \quad (12)$$

where dQ/dt is the flux determined from the amount transported (Q) over time (t) during the experiment, A is the surface area of the porous membrane, and C_o is the initial concentration in the donor side. P_{app} was determined from both experimental data and model predictions in the linear region of transport.

RESULTS

Effect of AP Uptake and P-gp-Mediated Efflux on the Cellular Accumulation and Absorptive Transport of Ranitidine in Caco-2 Cells

As shown in the accompanying paper, cation-selective AP uptake transporters and P-gp play an important role in the absorptive transport of ranitidine (1) and the associated kinetic parameters for AP ranitidine uptake are displayed in Table I. To determine the effect of AP uptake transporters and P-gp on the cellular kinetics of ranitidine, the absorptive transport and cellular accumulation of ranitidine (0.1 mM) were evaluated in Caco-2 cells in the absence or presence of the P-gp inhibitor GW918 (1 μM) or quinidine (200 μM), which is a dual inhibitor of cation-selective AP uptake transporters and P-gp. In the presence of GW918, the cellular accumulation and overall transport of ranitidine increased significantly compared to control (Fig. 2A, B). In the presence

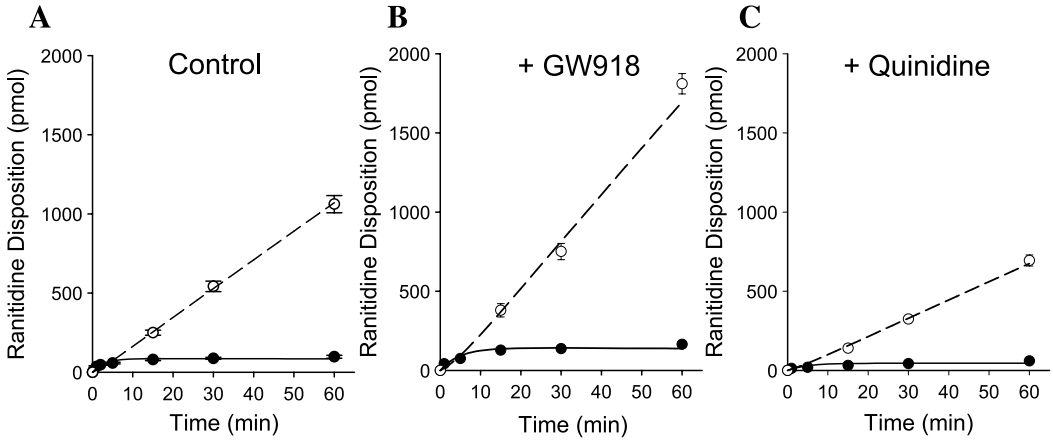

Fig. 2. Effect of AP uptake and efflux inhibition on the time course of ranitidine absorptive transport and cellular accumulation in Caco-2 cells. Ranitidine (0.1 mM) appearance in the BL compartment (○) and cellular accumulation (●) were monitored as a function of time in the absence (A) or presence of GW918 (1 μM) (B) and quinidine (200 μM) (C). Lines indicate the best fit of the kinetic model (Fig. 1) to the ranitidine BL appearance (dashed) and cellular accumulation (solid) data. Data represent mean ± SD; $n = 3$.

Table II. Kinetic Parameters Obtained from Nonlinear Least-squares Regression of Ranitidine Absorptive Transport and Cellular Accumulation Data in Caco-2 Cells

	Control		+GW918		+Quinidine	
Parameter	Estimate (min^{-1})	CV%	Estimate (min^{-1})	CV%	Estimate (min^{-1})	CV%
k_{12}	0.000750	n/a[a]	0.000750	n/a[a]	0.000235	29
k_{21}	0.254	20	0.0793	82	0.117	61
k_{23}	0.0869	60	0.126	69	0.0869	n/a[b]
k_{13}	0.000274	37	0.000305	69	0.000192	9

Data were fit simultaneously using the model equations detailed in "Materials and methods". k_{32} (0.0000417 min^{-1}) was fixed during modeling of all data sets using the kinetic parameters derived from initial ranitidine BL uptake data (12). n/a: not applicable.
[a] k_{12} was fixed during modeling of control and GW918 data sets using kinetic parameters derived from initial ranitidine AP uptake data (1).
[b] k_{23} was fixed during modeling of the quinidine data set at the parameter estimate obtained under control conditions.

of quinidine, however, the cellular accumulation and overall transport of ranitidine decreased significantly compared to control (Fig. 2A, C).

Kinetic modeling of the transport and accumulation data from the model scheme depicted in Fig. 1 yielded parameter estimates that described the ranitidine transport and accumulation data in the absence or presence of the uptake and efflux modulators (Table II). Based on previously determined experimentally derived kinetic parameters for AP ranitidine uptake (Table I) (1), the rate constant associated with AP uptake (k_{12}) was calculated and fixed at 0.000750 min^{-1} during modeling of data in the absence and presence of GW918. Preliminary experiments demonstrated that GW918 does not significantly affect the ranitidine initial AP uptake rate at the time point utilized to recover the kinetic parameters associated with ranitidine AP uptake (2 min) (data not shown) (1). Quinidine, however, significantly reduces the initial ranitidine AP uptake rate (1), and thus k_{12} was allowed to float during modeling of data in the presence of quinidine. The rate constant associated with BL efflux (k_{23}) was fixed at the parameter estimate obtained from the control ranitidine data set during analysis of the data obtained in the presence of quinidine. Ranitidine BL efflux data suggest that application of quinidine (200 μM) to the AP side of Caco-2 cells does not reduce the BL efflux of ranitidine (data not shown). The correspondence of the model to the data is presented in Fig. 2A–C. In the presence of GW918, the rate constant associated with AP efflux (k_{21}) decreased approximately 70%, consistent with inhibition of P-gp-mediated efflux of ranitidine (Table II). No obvious changes were observed in the rate constants associated with BL efflux (k_{23}) or paracellular transport (k_{13}) under these conditions (Table II). In the presence of quinidine, the parameter associated with AP ranitidine uptake (k_{12}) decreased by approximately 70%, consistent with the inhibition of AP uptake previously observed (1) (Table II). The AP efflux parameter (k_{21}) also decreased significantly in the presence of quinidine, suggesting that quinidine modulates ranitidine efflux as well (Table II). A slight decrease in the paracellular rate constant (k_{13}) was observed in the presence of quinidine (Table II).

Relative Contribution of Transcellular and Paracellular Transport Pathways to Ranitidine Absorptive Transport

The contribution of the transcellular and paracellular pathways to the overall absorptive transport of ranitidine was simulated based on the parameter estimates obtained from

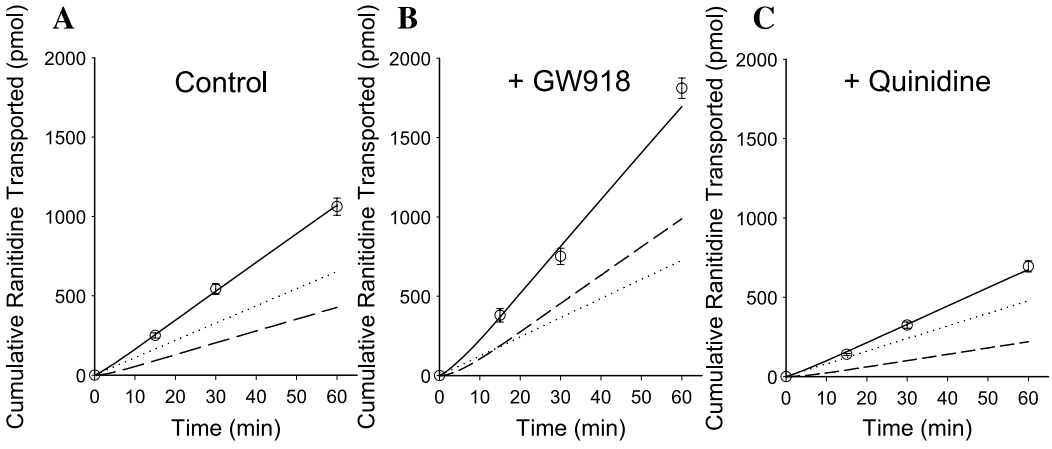

Fig. 3. Simulation of paracellular and transcellular contribution to ranitidine absorptive transport in the absence or presence of AP uptake and efflux inhibition in Caco-2 cells. Ranitidine (0.1 mM) appearance in the BL compartment (○) was monitored as a function of time in the absence (A) or presence of GW918 (1 μM) (B) and quinidine (200 μM) (C). Regression line (solid) indicates the best fit of the kinetic model (Fig. 1) to the ranitidine BL appearance data. Predicted ranitidine amount transported for transcellular (dashed line) and paracellular (dotted line) components of ranitidine absorptive transport were determined using subsets of the overall kinetic model and the parameter estimates displayed in Table II. Data represent mean ± SD; $n = 3$.

Table III. Relative Contribution of Paracellular and Transcellular Transport to Overall Absorptive Transport of Ranitidine in the Absence or Presence of AP Uptake and Efflux Inhibitors in Caco-2 Cells

	Model Prediction					Experimental
	$P_{app,\ total}$[a] (cm s^{-1}) $\times 10^7$	$P_{app,\ trans}$[b] (cm s^{-1}) $\times 10^7$	$P_{app,\ para}$[b] (cm s^{-1}) $\times 10^7$	% Transcellular[c]	% Paracellular[c]	$P_{app,\ total}$ (cm s^{-1}) $\times 10^7$
Control	30.2	12.4	18.1	40	60	30.0 ± 2.9
+GW918	49.2	29.7	20.1	60	40	53.8 ± 4.4
+Quinidine	19.2	6.6	13.2	30	70	20.5 ± 0.9

[a] Determined from the model prediction of total ranitidine transported as a function of time.
[b] Determined from simulation of amount of ranitidine transported as a function of time using a subset of the overall kinetic model incorporating solely paracellular or transcellular transport.
[c] Determined from the predicted paracellular or transcellular permeability as a percentage of the total predicted permeability.

kinetic modeling (Table II). Simulations utilized subsets of the original kinetic model that incorporated solely transcellular or paracellular kinetic events as described by Eqs. (7)–(11). In the absence of any transport modulators (control), absorptive transport of ranitidine (0.1 mM) was composed of significant paracellular and transcellular components (Fig. 3A). Paracellular transport of ranitidine was estimated to comprise approximately 60% of the total permeability for ranitidine ($P_{app,\ total}$) (0.1 mM) under control conditions (Table III; Fig. 3A). In the presence of GW918 (1 μM), the relative contribution of each pathway to ranitidine absorptive transport was shifted such that the transcellular contribution composed ~60% of the total permeability (Table III; Fig. 3B). As expected, the predicted transcellular permeability ($P_{app,\ trans}$) increased under these conditions, whereas the predicted paracellular permeability ($P_{app,\ para}$) exhibited little change (Table III). In the presence of quinidine (200 μM), a shift toward a predominant paracellular contribution (~70%) to ranitidine absorptive transport was observed (Table III; Fig. 3C). Quinidine caused a substantial decrease in the $P_{app,\ trans}$ as well as some decrease in the $P_{app,\ para}$, although the paracellular decrease was less than the transcellular decrease (Table III). Under all conditions, $P_{app,\ total}$ was similar whether determined from experimental data or predicted from the model (Table III).

Concentration Dependence of Ranitidine Absorptive Transport

The absorptive transport and cellular accumulation of ranitidine also were evaluated as a function of ranitidine concentration. The K_m for ranitidine absorptive transport and uptake are ~0.4–0.5 mM (1,4). Ranitidine concentrations utilized in this study were 0.1 mM (below K_m), 0.5 mM (~K_m), and 2 mM (above K_m). Consistent with a significant contribution from saturable absorptive transport, absorptive P_{app} of ranitidine decreased with increasing concentration. P_{app} values at 0.1, 0.5, and 2.0 mM were (33.1 ± 3.1) $\times 10^{-7}$, (21.2 ± 1.5) $\times 10^{-7}$, and (11.6 ± 2.5) $\times 10^{-7}$ cm s^{-1}, respectively. In addition, steady-state ranitidine cellular accumulation did not increase proportionally with ranitidine concentration. Accumulation of ranitidine at 2 mM was approximately 7-fold higher than that observed at 0.1 mM despite the 20-fold increase in initial donor concentration.

Kinetic modeling of ranitidine transport and accumulation data yielded parameter estimates that described the transport and accumulation data (Table IV). The fit of the model to the observed data is presented in Fig. 4A–C. Because increasing donor concentrations were expected to saturate AP uptake (k_{12}), k_{12} was not fixed in modeling of these data sets. Rather, the BL efflux parameter (k_{23}) was fixed for each concentration at the value previously esti-

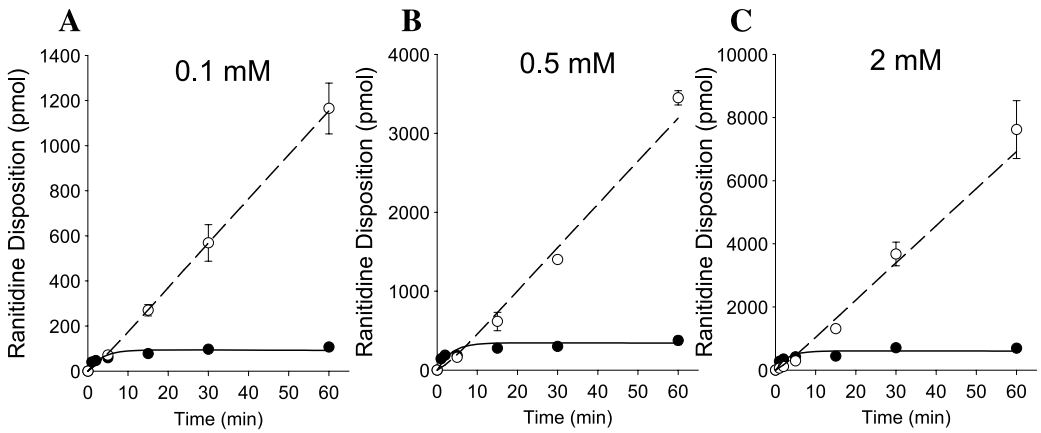

Fig. 4. Effect of donor concentration on the time course of ranitidine absorptive transport and cellular accumulation in Caco-2 cells. Ranitidine appearance in the BL compartment (○) and cellular accumulation (●) were monitored as a function of time after dosing of 0.1 (A), 0.5 (B), or 2.0 mM (C) ranitidine in the AP chamber. Lines indicate the best fit of the kinetic model (Fig. 1) to the ranitidine BL appearance (dashed line) and cellular accumulation (solid line) data. Data represent mean ± SD; $n = 3$.

Table IV. Kinetic Parameters Obtained from Nonlinear Least-squares Regression of Ranitidine Absorptive Transport and Cellular Accumulation Data as a Function of Concentration in Caco-2 Cells

	Donor concentration					
	0.1 mM		0.5 mM		2.0 mM	
Parameter	Estimate (min^{-1})	CV%	Estimate (min^{-1})	CV%	Estimate (min^{-1})	CV%
k_{12}	0.000693	22	0.000500	43	0.000267	33
k_{21}	0.205	35	0.200	66	0.264	51
k_{23}	0.0869	n/a[a]	0.0869	n/a[a]	0.0869	n/a[a]
k_{13}	0.000294	6	0.000126	15	0.000082	14

Data were fit simultaneously using the model equations detailed in "Materials and methods". k_{32} (0.0000417 min^{-1}) was fixed during modeling of all data sets using the kinetic parameters derived from initial ranitidine BL uptake data (12).
[a] k_{23} was fixed during modeling at the parameter estimate obtained under control conditions in Table II. n/a: not applicable.

mated under control conditions (0.0869 min^{-1}; Table II). Experimental BL efflux data suggested that the ranitidine BL efflux clearance did not saturate over a wide range of intracellular concentrations, and thus k_{23} would not be expected to change with increasing donor concentration (1). The rate constant associated with AP uptake (k_{12}) decreased with increasing ranitidine concentration, consistent with a saturable AP uptake mechanism (Table IV). No significant changes were observed in the rate constant for AP efflux (k_{21}) (Table IV). Interestingly, the estimated rate constant for paracellular transport (k_{13}) also decreased with increasing ranitidine concentrations (Table IV).

Relative Contribution of Transcellular and Paracellular Transport Pathways to Concentration-Dependent Ranitidine Absorptive Transport

Because AP uptake of ranitidine has been demonstrated to be nonlinear in Caco-2 cells, the relative contribution of the transcellular or paracellular route may be expected to change as a function of ranitidine concentration. However, no significant changes were observed in the relative contribution of the transcellular *vs.* paracellular route for ranitidine absorptive transport at ranitidine donor concentrations of 0.1 and 2.0 mM (~40% transcellular/~60% paracellular) (Table V; Fig. 5). Both the predicted $P_{app,\ trans}$ and predicted $P_{app,\ para}$ decreased significantly with increasing ranitidine concentration (Table V). A similar decrease (~70%) in the predicted $P_{app,\ para}$ and $P_{app,\ trans}$ was observed at the saturating concentration of 2.0 mM. However, the magnitude of the decrease observed in the $P_{app,\ para}$ was greater than the observed decrease in the $P_{app,\ trans}$ between 0.1 and 0.5 mM, resulting in the small shift to a higher transcellular contribution at 0.5 mM (Table V; Fig. 5B). The $P_{app,\ total}$ was again similar whether determined from experimental data or predicted from the model for each concentration (Table V).

DISCUSSION

A recent investigation of ranitidine absorptive transport in Caco-2 cells suggested a role for a carrier-mediated uptake process and P-gp-mediated efflux in the overall absorptive transport of ranitidine (1). Previous studies, however, have suggested that ranitidine absorptive transport is primarily mediated via the paracellular route (2–4). To evaluate the importance of each pathway to ranitidine absorptive transport, a quantitative analysis of the relative contribution of the transcellular and paracellular route is required. A relatively simple three-compartment kinetic model was utilized to estimate the relative contribution from each pathway. This approach incorporates the kinetics of cellular drug uptake and efflux as well as the kinetics of paracellular transport. The simultaneous nonlinear regression of cellular accumulation and transmonolayer transport data should provide a more accurate and quantitative determination of the relative transport pathways than previous methods based upon transport data alone.

Kinetic modeling of the ranitidine accumulation and transport data revealed significant parallel contributions of

Table V. Relative Contribution of Paracellular and Transcellular Transport to Overall Absorptive Transport of Ranitidine as a Function of Concentration in Caco-2 Cells

	Model Prediction					Experimental
Concentration (mM)	$P_{app,\ total}$[a] (cm/sec^{-1}) × 10^7	$P_{app,\ trans}$[b] (cm/sec^{-1}) × 10^7	$P_{app,\ para}$[b] (cm/sec^{-1}) × 10^7	% Transcellular[c]	% Paracellular[c]	$P_{app,\ total}$ (× 10^7 cm/sec^{-1})
0.1	32.6	13.6	19.4	40	60	33.1 ± 3.1
0.5	18.2	10.0	8.4	55	45	21.2 ± 1.5
2.0	9.8	4.4	5.4	45	55	11.6 ± 2.5

[a] Determined from the model prediction of total ranitidine transported as a function of time.
[b] Determined from simulation of amount of ranitidine transported as a function of time using a subset of the overall kinetic model incorporating solely paracellular or transcellular transport.
[c] Determined from the predicted paracellular or transcellular permeability as a percentage of the total predicted permeability.

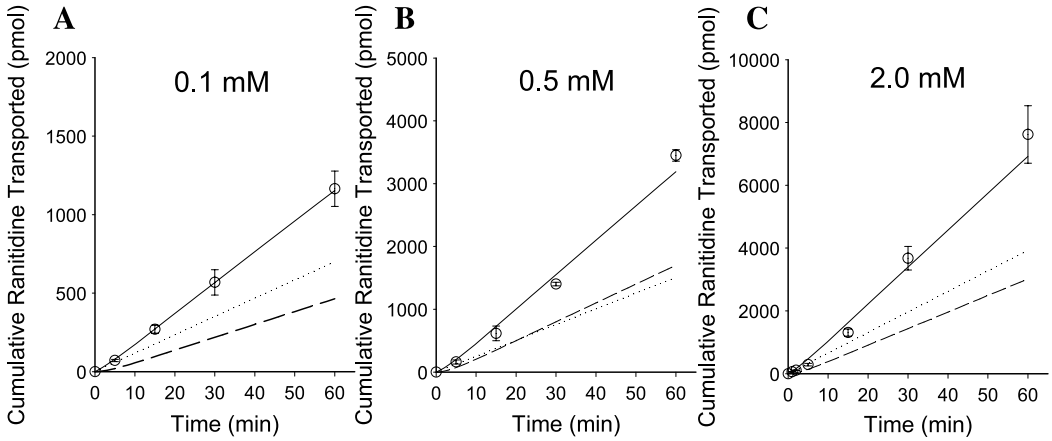

Fig. 5. Simulation of paracellular and transcellular contribution to ranitidine absorptive transport as a function of concentration in Caco-2 cells. Ranitidine appearance in the BL compartment (○) was monitored as a function of time after dosing of 0.1 (A), 0.5 (B), or 2.0 mM (C) ranitidine in the AP chamber. Solid line indicates the best fit of the kinetic model (Fig. 1) to the ranitidine BL appearance data. Predicted ranitidine amount transported for transcellular (dashed line) and paracellular (dotted line) components of ranitidine absorptive transport were determined using subsets of the overall kinetic model and the parameter estimates displayed in Table IV. Data represent mean ± SD; $n = 3$.

the transcellular and paracellular pathways to the absorptive transport of ranitidine. In the presence of intact uptake and efflux transporter mechanisms, approximately 40% of the overall ranitidine transport at 0.1 mM is expected to occur via the transcellular pathway, whereas approximately 60% would occur via the paracellular route (Tables III and V). The modeling also highlighted the interplay between absorptive transporter-mediated uptake and P-gp-mediated efflux across the AP membrane in the overall absorptive transport of ranitidine. Inhibition of P-gp-mediated ranitidine efflux resulted in the expected increase in ranitidine cellular accumulation and overall transport as well as a model-predicted upward shift in the relative contribution of the transcellular pathway (60% transcellular/40% paracellular) (Table III). This observed shift primarily reflects the decreased rate constant for AP efflux (k_{21}) (Table II) because no significant differences were observed in the rate constants for either BL efflux (k_{23}) or paracellular transport (k_{13}). Analysis of the model-predicted $P_{app,para}$ and $P_{app,trans}$ in the absence and presence of GW918 underscores the role of P-gp as a barrier to transcellular transport and its role in shifting some of ranitidine's absorptive transport toward the paracellular route. Inhibition of P-gp resulted in an approximately 2.5-fold increase in the predicted $P_{app,trans}$ of ranitidine (Table III). However, the overall predicted $P_{app,total}$ increased only 1.6-fold due in large part to the significant paracellular contribution to overall transport under both conditions (Table III). Such discrepancies between the observed increases in $P_{app,trans}$ and $P_{app,total}$ after P-gp inhibition for hydrophilic P-gp substrates such as ranitidine are consistent with a significant paracellular component to its absorptive transport.

Quinidine significantly reduces ranitidine accumulation in Caco-2 cells through potent inhibition of AP ranitidine uptake (IC_{50} ~10 μM) (1). Quinidine, however, also inhibits P-gp in Caco-2 cells (13). In the presence of quinidine (200 μM), the cellular accumulation and absorptive transport of ranitidine in the current study were reduced significantly compared to control (Fig. 2A, C). The rate constants associated with both AP uptake (k_{12}) and efflux (k_{21}) decreased markedly compared to control, consistent with inhibition of both the carrier-mediated uptake and P-gp-mediated efflux of ranitidine (Table II). Because both uptake and efflux likely are inhibited completely at the quinidine concentrations used in the study, the data suggest that the uptake process clearly seems to have a more significant effect upon the intracellular accumulation of ranitidine. Furthermore, the reduced uptake of ranitidine results in a significant shift to the paracellular route (~70%) for ranitidine transport under these conditions. These results suggest that hydrophilic drugs utilizing carrier-mediated absorption mechanisms may exhibit varying contributions from the transcellular and paracellular pathways depending on the activity/

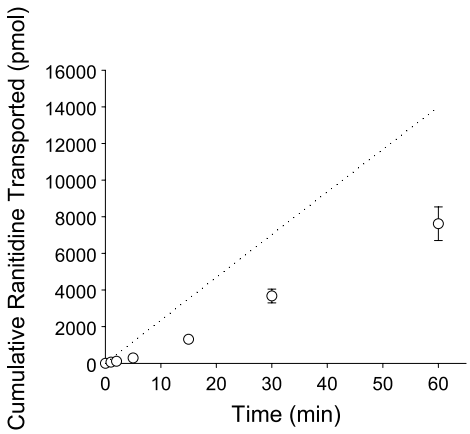

Fig. 6. Simulation of paracellular contribution to ranitidine (2.0 mM) absorptive transport in Caco-2 cells. Ranitidine appearance in the BL compartment (○) was monitored as a function of time. Dotted line indicates the predicted ranitidine amount transported for the paracellular component of ranitidine absorptive using a subset of the overall kinetic model and a fixed paracellular (k_{13}) parameter estimate of 0.000294 min^{-1} determined at 0.1 mM.

efficiency as well as inhibition/induction of uptake and efflux transporters involved in their overall transport.

Previous studies have demonstrated size- and charge-dependent paracellular permeability of hydrophilic solutes, with cationic solutes displaying higher paracellular permeabilities than neutral or anionic solutes of similar molecular radius (5,14). The kinetic model employed in the present study predicted a paracellular permeability of 10–20 $\times 10^{-7}$ cm s^{-1} at 0.1 mM for the organic cation ranitidine in Caco-2 cells (Tables III and V). Although this permeability coefficient is larger than that typically observed for a neutral paracellular permeant such as mannitol [~(3–5) $\times 10^{-7}$ cm s^{-1}], it is in good agreement with the reported paracellular permeability of other hydrophilic cations of similar size and charge, such as atenolol (16.7 $\times 10^{-7}$ cm s^{-1}) (14). Interestingly, a slight decrease in both the paracellular rate constant (k_{13}) and the predicted $P_{app,\ para}$ of ranitidine was observed in the presence of the organic cation quinidine (Tables II and III). This may suggest some inhibition of ranitidine transport within the paracellular space by quinidine, possibly due to charge–charge interaction between cationic molecules and anionic residues as previously postulated (4).

A decrease in the rate constants for both AP uptake (k_{12}) and paracellular transport (k_{13}) also was observed as the initial ranitidine concentration in the donor compartment was increased (Table IV). Subsequently, this led to an observed decrease in both the predicted $P_{app,\ trans}$ and predicted $P_{app,\ para}$ for ranitidine absorptive transport (Table V). It was expected that k_{12} and $P_{app,\ trans}$ would decrease based on the saturable experimental uptake data (1). However, the effect of increasing concentration upon k_{13} and $P_{app,\ para}$ was largely unknown. The observed decrease in k_{13} and $P_{app,\ para}$ is consistent with a saturable paracellular transport mechanism for ranitidine (4). Recent evidence suggesting that anionic amino acid residues of claudins confer cationic charge selectivity to the paracellular pathway (15) supports a model of saturable interaction between cationic drugs and anionic amino acid residues in tight junctional proteins. Piyapolrungroj *et al.* (16) and Zhou *et al.* (17) have hypothesized, based on rat intestinal perfusion studies with a related H_2 receptor antagonist, cimetidine, that it may restrict its own absorption via the paracellular route as a result of paracellular constriction stemming from increased intracellular cimetidine concentrations at high perfusate (donor) concentrations. A similar mechanism operative in Caco-2 cells could also explain the observed data for ranitidine in the present study. It has been demonstrated previously that increased donor concentrations of ranitidine result in increased TEER values across the monolayers (4,18). However, high donor concentrations of H_2 receptor antagonists do not seem to regulate the paracellular space in Caco-2 cells, as the flux of paracellular markers such as mannitol is not significantly affected in their presence (4). The observed decrease in the paracellular rate constant also probably is not an artifact of the modeling process. Fixing the paracellular rate constant at the value obtained at 0.1 mM (0.000294 min^{-1}) resulted in an overestimation of ranitidine absorptive transport at 2.0 mM, suggesting a decrease is required in this parameter to accurately fit the model to experimental data (Fig. 6). Although the exact mechanism underlying this decrease remains unclear, the modeling results support a hypothesis in which paracellular absorption of ranitidine is reduced at high donor concentrations possibly as a result of a saturable paracellular transport pathway. It remains to be determined if the saturable paracellular transport mechanism can be demonstrated for other hydrophilic cations such as cimetidine, famotidine, atenolol, and metformin. The approach used for ranitidine may also be applied to these compounds to determine if saturable paracellular transport is a general transport mechanism that applies to diverse hydrophilic cations.

Considering that the paracellular permeability in Caco-2 cells is generally lower than that observed in human intestine (19), the paracellular route may contribute even more to overall ranitidine absorption *in vivo* than that suggested from the predicted relative paracellular contribution derived in Caco-2 cells. However, differences in the contribution and expression of the organic cation uptake system between Caco-2 and human intestine also likely exist, rendering an extrapolation of the relative contribution of each pathway to human absorption difficult. Despite these limitations, the present kinetic modeling study, in conjunction with the previous observations on the role of absorptive organic cation transporters involved in the AP uptake of ranitidine in Caco-2 cells (1) suggests a role for saturable transport processes in the oral absorption of ranitidine. Such a mechanism may explain the observed high bioavailability of this hydrophilic compound in humans. Interestingly, a clinical study designed to investigate if oral absorption of ranitidine is saturable clearly established the presence of a saturable component in the intestinal absorption of this drug (20). Whether the saturable paracellular transport mechanism exists in human intestine remains to be determined because direct evidence to link the *in vitro* studies and modeling of ranitidine transport in the Caco-2 system with its intestinal absorption in humans is still lacking.

Although the focus of the current study is the relative contribution of transcellular and paracellular transport to the absorptive transport of ranitidine, the kinetic modeling approach developed in this study will complement the currently available methods to estimate paracellular and transcellular transport and may be generally applicable for the estimation of the relative contribution of paracellular and transcellular transport for other drugs. Its application may be especially useful and advantageous in situations where multiple, complex transport pathways such as those observed for ranitidine (i.e., active uptake, active efflux, and paracellular transport) exist in the overall transport of a molecule. The previously devised methods based on the theory of molecular-size-restricted diffusion (5–7) and combined PAMPA/Caco-2 data (8) remain convenient tools to assess the contribution of paracellular and transcellular transport especially for compounds whose predominant transport mechanism across the monolayers is via passive diffusion. Other methods also have been developed to assess the contribution of paracellular transport that may be more useful in mimicking the *in vivo* environment due to greater paracellular leakiness that is more reflective of the human intestine than Caco-2 cells (9). The appropriate method to assess paracellular and transcellular transport will thus likely depend on the complexity of drug transport involved and the assumptions that can be applied to a given situation. More importantly, the kinetic

modeling approach developed here incorporates the kinetics of cellular drug uptake and efflux in addition to the overall transepithelial transport data and thus achieves a more complete assessment of the role for each pathway than methods based solely on transepithelial transport data. This kinetic modeling approach may have application in estimating the impact of uptake and/or efflux transporter inhibition or induction by coadministered therapeutic agents during intestinal drug absorption and improve the ability to predict intestinal transporter-based drug–drug interactions.

ACKNOWLEDGMENTS

David L. Bourdet was supported by a Pharmaceutical Research and Manufacturers of America (PhRMA) Foundation predoctoral fellowship in pharmaceutics. The Caco-2 cell line was kindly provided by Drs. Mary F. Paine and Paul Watkins of the University of North Carolina at Chapel Hill.

REFERENCES

1. D. L. Bourdet and D. R. Thakker. Saturable absorptive transport of the hydrophilic organic cation ranitidine in caco-2 cells: role of pH-dependent organic cation uptake system and P-glycoprotein. *Pharm. Res.* **23**(6):1165–1177 (2006).
2. L. S. Gan, P. H. Hsyu, J. F. Pritchard, and D. Thakker. Mechanism of intestinal absorption of ranitidine and ondansetron: transport across Caco-2 cell monolayers. *Pharm. Res.* **10**: 1722–1725 (1993).
3. A. Collett, N. B. Higgs, E. Sims, M. Rowland, and G. Warhurst. Modulation of the permeability of H_2 receptor antagonists cimetidine and ranitidine by P-glycoprotein in rat intestine and the human colonic cell line Caco-2. *J. Pharmacol. Exp. Ther.* **288**:171–178 (1999).
4. K. Lee and D. R. Thakker. Saturable transport of H_2-antagonists ranitidine and famotidine across Caco-2 cell monolayers. *J. Pharm. Sci.* **88**:680–687 (1999).
5. A. Adson, T. J. Raub, P. S. Burton, C. L. Barsuhn, A. R. Hilgers, K. L. Audus, and N. F. Ho. Quantitative approaches to delineate paracellular diffusion in cultured epithelial cell monolayers. *J. Pharm. Sci.* **83**:1529–1536 (1994).
6. A. Adson, P. S. Burton, T. J. Raub, C. L. Barsuhn, K. L. Audus, and N. F. Ho. Passive diffusion of weak organic electrolytes across Caco-2 cell monolayers: uncoupling the contributions of hydrodynamic, transcellular, and paracellular barriers. *J. Pharm. Sci.* **84**:1197–1204 (1995).
7. V. Pade and S. Stavchansky. Estimation of the relative contribution of the transcellular and paracellular pathway to the transport of passively absorbed drugs in the Caco-2 cell culture model. *Pharm. Res.* **14**:1210–1215 (1997).
8. R. Saitoh, K. Sugano, N. Takata, T. Tachibana, A. Higashida, Y. Nabuchi, and Y. Aso. Correction of permeability with pore radius of tight junctions in Caco-2 monolayers improves the prediction of the dose fraction of hydrophilic drugs absorbed by humans. *Pharm. Res.* **21**:749–755 (2004).
9. N. Nagahara, S. Tavelin, and P. Artursson. Contribution of the paracellular route to the pH-dependent epithelial permeability to cationic drugs. *J. Pharm. Sci.* **93**:2972–2984 (2004).
10. P. Schmiedlin-Ren, K. E. Thummel, J. M. Fisher, M. F. Paine, K. S. Lown, and P. B. Watkins. Expression of enzymatically active CYP3A4 by Caco-2 cells grown on extracellular matrix-coated permeable supports in the presence of 1alpha,25-dihydroxyvitamin D3. *Mol. Pharmacol.* **51**:741–754 (1997).
11. F. Hyafil, C. Vergely, P. Du Vignaud, and T. Grand-Perret. *In vitro* and *in vivo* reversal of multidrug resistance by GF120918, an acridonecarboxamide derivative. *Cancer. Res.* **53**:4595–4602 (1993).
12. K. Lee, C. Ng, K. L. R. Brouwer, and D. R. Thakker. Secretory transport of ranitidine and famotidine across Caco-2 cell monolayers. *J. Pharmacol. Exp. Ther.* **303**:574–580 (2002).
13. M. F. Fromm, R. B. Kim, C. M. Stein, G. R. Wilkinson, and D. M. Roden. Inhibition of P-glycoprotein-mediated drug transport: a unifying mechanism to explain the interaction between digoxin and quinidine. *Circulation* **99**:552–557 (1999).
14. G. T. Knipp, N. F. Ho, C. L. Barsuhn, and R. T. Borchardt. Paracellular diffusion in Caco-2 cell monolayers: effect of perturbation on the transport of hydrophilic compounds that vary in charge and size. *J. Pharm. Sci.* **86**:1105–1110 (1997).
15. O. R. Colegio, C. M. Van Itallie, H. J. McCrea, C. Rahner, and J. M. Anderson. Claudins create charge-selective channels in the paracellular pathway between epithelial cells. *Am. J. Physiol. Cell Physiol.* **283**:C142–C147 (2002).
16. N. Piyapolrungroj, Y. S. Zhou, C. Li, G. Liu, E. Zimmermann, and D. Fleisher. Cimetidine absorption and elimination in rat small intestine. *Drug Metab. Dispos.* **28**:65–72 (2000).
17. S. Y. Zhou, N. Piyapolrungroj, L. Pao, C. Li, G. Liu, E. Zimmermann, and D. Fleisher. Regulation of paracellular absorption of cimetidine and 5-aminosalicylate in rat intestine. *Pharm. Res.* **16**:1781–1785 (1999).
18. L. S. Gan, S. Yanni, and D. R. Thakker. Modulation of the tight junctions of the Caco-2 cell monolayers by H2-antagonists. *Pharm. Res.* **15**:53–57 (1998).
19. P. Artursson, A. L. Ungell, and J. E. Lofroth. Selective paracellular permeability in two models of intestinal absorption: cultured monolayers of human intestinal epithelial cells and rat intestinal segments. *Pharm. Res.* **10**:1123–1129 (1993).
20. C. M. Brandquist, C. Ng, D. R. Thakker, and K. L. Brouwer. Novel interactions in the oral absorption of hydrophilic cations: a clinical study with ranitidine and famotidine. *Clin. Pharmacol. Ther.* **73**:19 (2003).